The Design and Validation of a Folded Dipole Antenna with a Corner Reflector

Simo Gabriel, Jasper Jonker, Jules van Liefland, Nehal Mathur, Duc Tan Nguyen, Samuel Oyediran, Jasper Ringoot, Jasper van der Schaaf, Jeroen Schlief and Andrea Veciana Picazo

***Abstract*—The aim of this paper is to present a design for a folded dipole antenna with a corner reflector and verify the design through simulations and experiments. COMSOL MultiPhysics is used to simulate the gain of the system and optimal distance of the dipole with respect to the reflector. Using Realtek 2832u USB Dongle, experiments were done to measure the impedance and gain of the antenna. A comparison between the simulations and experiments tells that the antenna is far from ideal, but a signal was still retrieved.**

I. Introduction

THE purpose of this report is to display our finding on the design, working and construction of an antenna that is able to transmit at a frequency of 433MHz at a distance of 100m with a signal which should be as strong as possible. In this report, we will be focusing on the half wave folded dipole in combination with a corner reflector. Starting with a theoretical analysis of the antenna of the corner reflector, the required dimensions needed for both to acquire the desired transmission where calculated analytically. Next, simulations where done to verify the theoretical findings and adjust for a more practical situation. Finally the designed antenna was tested experimentally. Trough the model and measurements, the design of the folded dipole antenna with a corner reflector will be discussed and validated.

II. Operation Principles

A. Folded Dipole

A folded dipole can be represented as two dipoles with a length of $\lambda/2$ that are joined together at the extremities. The transmission line is located at the center of one of the dipoles. A model of the folded dipole can be derived by starting with a Hertzian dipole and then adding components to the system to adapt the model into a linear dipole, then half wave dipole and finally folded dipole. Assumptions are made to simplify the theory into a viable model: the side parts where the dipole is folded are neglected, the separation distance is not larger than 1 wavelength and the electric and magnetic field decrease linearly with the separation distance. The directivity is the ratio of the radiation intensity in a given direction from the antenna to the radiation intensity averaged over all directions. As seen in equation 1 [2].

$$D(\theta,\phi) = \frac{P(r,\theta,\phi)}{P_R/4\pi r^2} \tag{1}$$

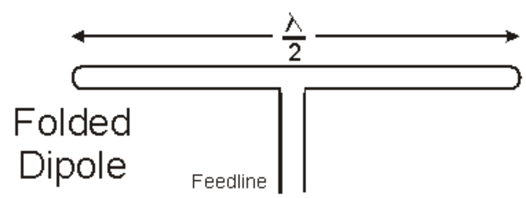

Fig. 1. Schematic of folded dipole [1]

The total power is obtained by integrating the radiation intensity over the entire solid angle of 4π. Thus:

$$P(\theta,\phi)_{av} = \frac{1}{4\pi}\int_0^{2\pi}\int_0^{\pi} P(\theta,\phi) sin\theta d\theta d\phi \tag{2}$$

$$P(\theta,\phi)_{av} = \frac{1}{4\pi}\int\int_{4\pi} P(\theta,\phi) d\Omega \tag{3}$$

Therefore, the directivity becomes:

$$D = \frac{1}{(1/4\pi)\int\int_{4\pi}[P(\theta,\phi)/P(\theta,\phi)_{max}]d\Omega} \tag{4}$$

If the radiation frequency is equal for all angles, then the directivity is:

$$D(\theta,\phi) = \frac{4\pi U(\theta,\phi)}{P_{rad}} \tag{5}$$

We begin by calculating the radiation intensity produced by the dipole:

$$U(\theta) = \frac{1}{2}r^2|E_\theta|^2 = 36.5640 I_m^2 \tag{6}$$

The maximum effective area is A_{em} and the maximum directivity relative to an isotopic radiator is then calculated as:

$$D_m = \frac{4\pi U_m}{P_{rad}} \approx 1.64 \approx 2.15\ dBi \tag{7}$$

B. Corner Reflector

A corner reflector consists of two conducting metal sheets connected at an angle, placed behind a dipole antenna. The addition of a corner reflector to a dipole results in an increased gain and directivity [3]. The conducting plates effectively work as two mirrors, thus creating multiple images of the feed antenna, all adding to the intensity of the antenna, as can be seen in figure 2. Image #4 is in phase with the feed #1, while images #2 and #3 are 180° out of phase.

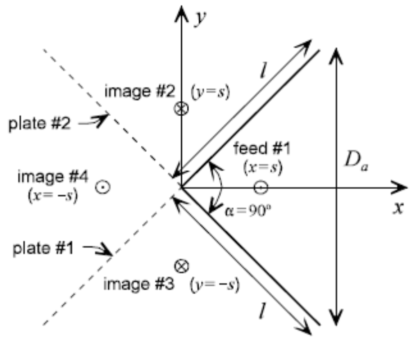

Fig. 2. The operating principle of a corner reflector [3]

The array factor is used to describe the radiation pattern of an array of antennas [4]. For a corner reflector antenna at a 90° angle this is:

$$AF = 2[\cos(ks\cos\theta) - \cos(ks\sin\theta)] \tag{8}$$

The operation principle of a corner reflector is described using image theory assuming infinite plates [5] [6] [7]. Therefore, for the exact dimensions of the reflector, conventions are used, backed by experimental data and simulations. Rather than conducting plates, a wire screen can be used. As long as the used frequency is below the cutoff frequency $\omega_c = \frac{\pi c}{a}$. Where a is the separation distance of the wiring [8].

C. Power cofficient

The power received from one antenna which was received from another antenna can be calculated by using Friis transmission equation:

$$\frac{P_r}{P_t} = G_t G_r \left(\frac{\lambda}{4\pi R}\right)^2 \tag{9}$$

where P_r and P_t are the power received and transmitted, respectively. G_r and G_t are the antenna gains [9]. If the gain has units of dB, then the equation can be rewritten as [10]:

$$P_R(d) = P_T + G_T + G_R + 10\log_{10}\left(\frac{\lambda}{4\pi d}\right)^n \tag{10}$$

The last term of the equation can be expanded to:

$$log_{10}\left(\frac{\lambda}{4\pi d}\right)^n = n\left[\log_{10}\lambda - \log_{10}(4\pi) - \log_{10} d\right] \tag{11}$$

and thus by using logarithmic properties this expression can be simplified to:

$$P_R(d) = C_{T,R} - 10n\log_{10} d \tag{12}$$

where the C coefficient contains:

$$C_{T,R} = P_T + G_T + G_R + 10log_{10}\left(\frac{\lambda}{4\pi}\right)^n \tag{13}$$

III. Antenna Design

A. Overview of Design

1) Folded Dipole: The chosen length of the folded dipole is $31\,\mathrm{cm}$ such that the total dipole length is 1 wavelength. The separation distance will be $2.6\,\mathrm{cm}$ as this has to be as small as possible and is believed to be the smallest possible distance that can be properly constructed.

A $75\,\Omega$ coax cable will be used to transmit the signal out of the signal box. The proper phase at both feed points can be obtained by attaching $\lambda/2$ extra wire length to one of the feed points. The $75\,\Omega$ coax cable has a much lower impedance than the folded dipole which can be fixed with the extra wire length.

The actual antenna has a dipole length of $29\,\mathrm{cm}$. This is because the separation between the dipoles is increased to $3.95\,\mathrm{cm}$, with a feedpoint gap of $3.0\,\mathrm{cm}$ brings this the total dipole length to $68.9\,\mathrm{cm}$. Although this is $0.1\,\mathrm{cm}$ shorter than the ideal length it is close enough to not have a significant impact.

2) Corner Reflector: The commonly used angle is 90° as larger angles result in fewer than three images, while smaller angles result in more. Since, smaller angles do not significantly increase the gain, these are not often used [5]. The height of the plates should be about 1.2 - 1.5 times larger than the folded dipole [3], therefore a height of $50\,\mathrm{cm}$ was chosen. Since the length of corner reflector is usually about one wavelength, it should be $69\,\mathrm{cm}$.

The chosen dimensions for the wire screen are based on the bird wire commercially available. The spacing of the wires is $12\,\mathrm{mm}$, while the thickness is $0.65\,\mathrm{mm}$ thus the cutoff frequency is $\omega_c = \frac{\pi c}{0.012} = 7.85 \cdot 10^{10}$, where $433\,\mathrm{MHz}$ is well below it.

The distance s of the folded dipole to the corner reflector usually is about half a wavelength [3][2]. The simulations in section IV-B find different values. The final distance s is empirically determined through experiments.

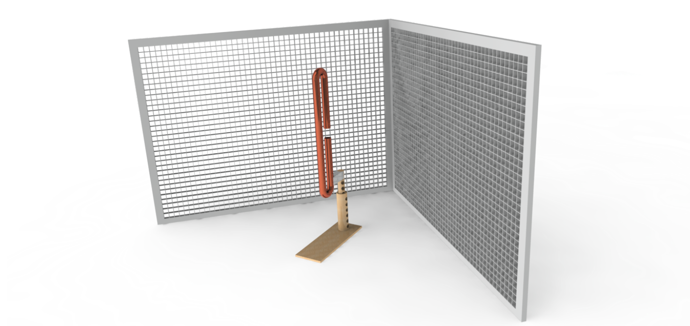

Fig. 3. Illustration of Folded Dipole with Corner Reflector

B. Construction

The technical drawings in the midterm report were used as basis for construction. The dipole had to be constructed with a hollow copper tube. The theoretically calculated radius was practically not possible by simply bending the tube. Instead corner pieces were placed to achieve an as small as possible distance between the two long sides of the folded dipole. These were attached by hard soldering the several pieces together. After that the appropriate wires were soldered onto the ends of the dipole. In the table below one can see a comparison between the theoretical dimensions and the dimensions after building:

Length measured	**Theoretical**	**Construction**
Current feed gap	2.4 cm	3 cm
Top to bottom	31 cm	29 cm
Gap between dipoles	1.76 cm	2.2 cm
Tube diameter	1.70 cm	1.50 cm

The corner reflector was constructed with square bird wire and wood. From the dimensions in the technical drawings, the wooden frame was cut, which was held together with staples and glue. After construction of the frame one piece of bird wire was stapled onto both frames. With the bird wire acting as a hinge so that the corner reflectors' angle could still be altered. The final dimensions after construction were identical to that of the theoretically calculated one.

IV. Simulations

A. Model Setup

To analyze the behavior of the system, simulations were done using Comsol. A folded dipole geometry (Figure 4) was setup and adjusted to the constructed specifications. Table I shows how the initial parameters were altered based on our construction as well as promising simulations.

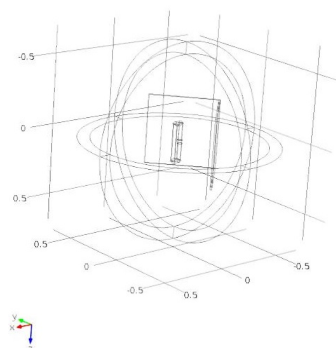

Fig. 4. Geometry Setup of a Folded Dipole including Corner Reflector

TABLE I
Table of Parameters

Parameter	Original Value (cm)	Final Value (cm)
Wavelength	69.3	N/A
Source Gap	2.4	3
Reflector Size	49·49	68·50
Wire Separation	5.16	2.2
Wire Radius	1.7	1.5
Length Long Side	26	28
Half Length Short Side	11.8	11.5
Distance to Reflector	34.65	17.325

B. Simulation Results

The simulated radiation patterns of our specific design can be seen in Figures 5 & 6. The 2D near field radiation pattern proves that the folded dipole is functioning properly as it indicates the expected current distribution shape. Figure 6 on the other hand proves that the corner reflector is fulfilling its function to focus the signal parallel to the geometry.

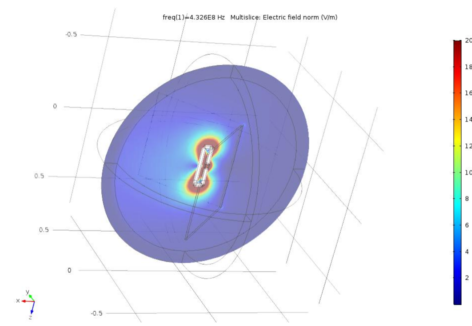

Fig. 5. 2D Near and Far Field Radiation Pattern, Electric Field Norm (V/m)

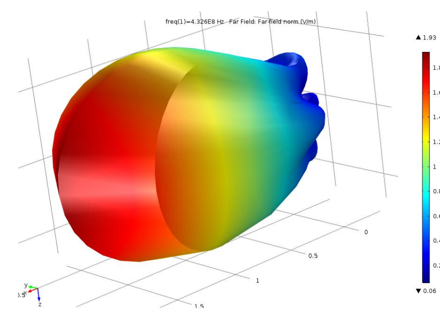

Fig. 6. 3D Far Field Radiation Pattern, Far Field Norm (V/m)

Using the working model, multiple parametric sweeps were performed on the source gap size, size of the reflector and the distance to the reflector. One such sweep's 2D directivity output can be seen in Figure 7. Observations from these simulations include the preference of a smaller gap size (1.5-2 cm), larger reflector and the distance from the reflector to be a quarter of the wavelength.

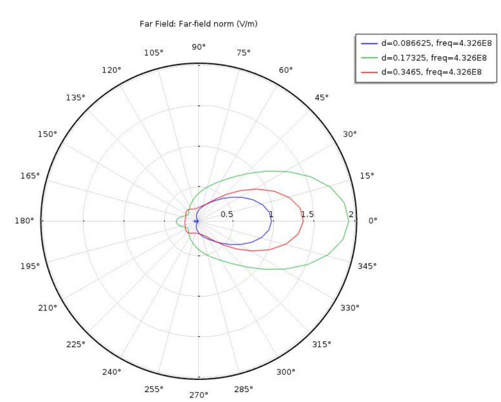

Fig. 7. 2D Far Field Norm (V/m) of a Distance to Reflector Parameter Sweep $\lambda/8$ in blue, $\lambda/4$ in green and $\lambda/2$ in red

V. Experiments

To validate that the antenna is working, measurements were done to retrieve information regarding the gain, directivity, power and influence of the corner reflector. The first tests were done inside to check if the software SDRsharp and the transmitter box worked.
The four main experiments that were done:

1) Measure the SNR of the folded dipole with and without the corner reflector by varying the distance between the receiver and source
2) At a fixed distance, measure the dBFS of the folded dipole while rotating the system about the x-axis
3) At a fixed distance, measure the dBFS of the folded dipole while rotating the system about the y-axis
4) Vary the distance between the corner reflector and the folded dipole

The overall setup of these experiments was a computer, running SDRsharp, connected to the Realtek 2832u USB which served as a receiver and a transmitter box was connected to the folded dipole. Distances and angles were marked on the floor in line with the receiver antenna. All of the measurements were taken outdoors to minimize the reflection of the waves.

The data retrieved for the first experiment can be seen in table II. The receiver was positioned at a fixed location and then the distance to the folded dipole was varied in steps of four meters. The signal to noise ratio and the peak were recorded for each distance. The same steps were repeated but now with the addition of the corner reflector. These measurements were done to analyze the power loss over distance and to observe the influence of the corner reflector to the overall system. Next,

TABLE II
Experiment 1: varying the distance between the folded dipole and the receiver with and without corner reflector

Distance [m]	SNR [dB]	SNR with reflector [dB]
4	51.66	59.9
8	40.7	45.5
12	38.4	45.9
16	36.6	37.5
20	31.1	38.7
24	31.2	37.9
28	25.0	39.9
32	32.0	32.1
36	29.8	39.6
40	22.4	31.9
44	20.6	31.5
48	21.3	29.9
52	16.8	30.6

experiments 2 and 3 were conducted to plot the horizontal and vertical radiation patterns. The antenna was rotated in steps of 20° and the peak was recorded respectively. Tables III and IV present the data retrieved.

Experiment 4 was conducted by placing the corner reflector at a fixed distance of four meters away from the reciever. The folded dipole was then placed at varying distances, the data obtained is represented in the table V.

A. Measurement Results

While testing the antenna and looking for a peak in the SDRsharp software, the frequency of the antenna was clearly

TABLE III
Experiment 2: At a distance of 4 meters, rotation about x-axis

Angle [°]	Signal [dBFS]
0	-15.3
20	-18.2
40	-20.5
60	-19.7
80	-21.1
100	-22.3
120	-22.7
140	-25.7
160	-28.4
180	-25.8
200	-21.5
220	-22.7
240	-23.2
260	-30.0
280	-34.9
300	-26.8
320	-31.8
340	-22.7
360	-15.6

TABLE IV
Experiment 3: At a distance of 4 meters, rotation about y-axis

Angle [°]	Signal [dBFS]
0	-11,2
20	-7,3
40	-0,5
60	-3,3
80	-13,3
100	-25
120	-15,5
140	-11,4
160	-20,4
180	-23,6
200	-24,8
220	-15,6
240	-8,7
260	-16,8
280	-30,3
300	-27,2
320	-25,8
340	-6,5
360	-11,2

seen at $433.9161\,\mathrm{MHz}$. Throughout the experiments, this frequency did not vary. Using equation 13, from section II-C a fit can be made to calculate the experimental power coefficient. As seen in figure V-A, the SNR values retrieved from experiment 1 were plotted against distance. The blue data points and fit represent the measurements done with the entire system, whereas the red curve represents the power decay of the folded dipole. The decay power for the dipole with corner reflector is determined to be 2.345, which is higher than the free space model where n = 2. Furthermore, the folded dipole has a power coefficient equal to 2.781, which is higher than that of the entire system. Concluding from these results (shown in table VI), the corner reflector increases the signal and decreases the power loss over distance.

From experiments 2 and 3 two polar plots (III,IV) were made representing the vertical and horizontal radiation patterns. The units are in decibels relative to full scale (dBFS), which means that at 0 dBFS the signal is maximum.

As stated in the theory of the corner reflector, the distance s between the corner reflector and the folded dipole is of high

TABLE V
EXPERIMENT 4: VARYING THE DISTANCE (S) BETWEEN THE CORNER REFLECTOR AND FOLDED DIPOLE

s [cm]	Signal [dBFS]
4 4	-3,5
9	1,1
14	0,7
29	0,2
24	5,7
29	5,5
34	5,4
39	4,9
44	5,6
49	6,6
54	5,9
59	4,8
64	4,9
69	2,9
74	-4
79	-7,2
84	-8,1
89	-9,9
94	-6,5
99	-4,5
104	-1

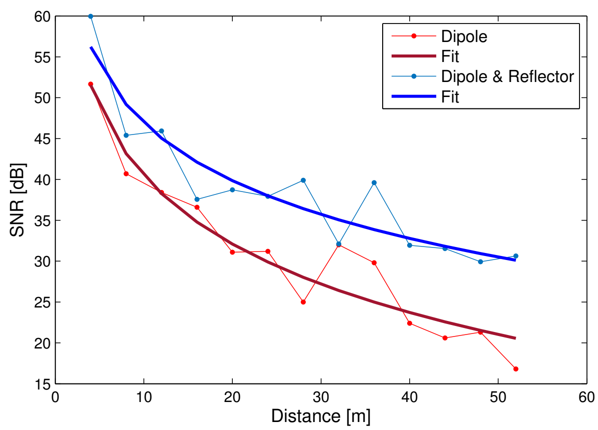

Fig. 8. Signal to Ratio versus distance of the folded dipole (red) and folded dipole with corner reflector (blue) with a fit of $y = c - 10nlog_{10}(x)$. The power coefficient, n, is determined through the fit.

importance to achieve maximum power. Experiment 4 was done by keeping the corner reflector at a distance of four meters from the receiver and then varying the distance of the folded dipole. This distance was taken from the corner of the reflector to the center of the dipole. The peak measured was plotted against the distance and after making a fit of $y = asin\,(bx + c)$, the optimal distance was found to be $40.08\,\mathrm{cm}$. Furthermore, from the graph V-A a sinusoidal behavior can be seen from the data points which indicates that there is both constructive and destructive interference.

VI. Comparison

A comparison can be drawn between simulations and measured results to further analyze what the strengths and flaws of the system are. Clearly, the outcome of the experiments does not match the expected outcome from the simulations.

TABLE VI
FIT PARAMETERS

n	c
2.345	70.34
2.781	68.28

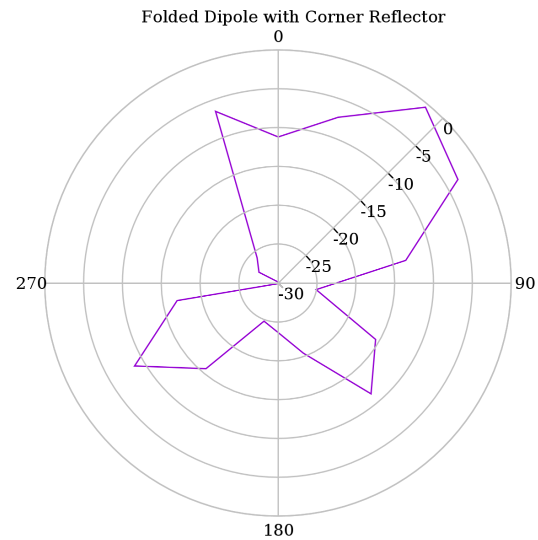

Fig. 9. Measured horizontal radiation pattern at a distance of $4\,\mathrm{m}$, where the signal is measured in dBFS

One of the first differences one can easily see is the difference in radiation patterns. The dipole alone should have an omnidirectional field according to the simulations [2], but in figure 10 one can conclude that the induced radiation is not omnidirectional. Another difference between simulations and experiments that can be noted is the effect of adding a corner reflector to the system. The outcome of the experiment with corner reflector (figure 9) clearly is not the same as the one found in the simulations (figure 6). According to the theory and simulations the corner reflector would increase the directivity in the 0° direction. From the experiments a certain increase in directivity is measured, however some of the power is radiated in unexpected directions.

Thankfully, some hypotheses made during the midterm report were confirmed by both the simulations and calculations. An example is the $1/r$ dependence in the far field for the signal strength as can be seen in figure 8. Another example is the sinusoidal behavior of the constructive and destructive interference pattern as can be found in figure 11. Finally, the distance s was found using both the simulations and experimental values. s Denotes the distance of the dipole from the corner reflector, which had a lot of influence on parameters such as gain. From the simulations a distance of $\lambda/4$ was found, but from experimental data a distance of 40.08cm ($\approx 0.58\lambda$) was found. Differences in simulated and experimental data are discussed below.

VII. Discussion

The most critical factors that needed to be validated for the designed antenna are the gain, directivity and the influence of

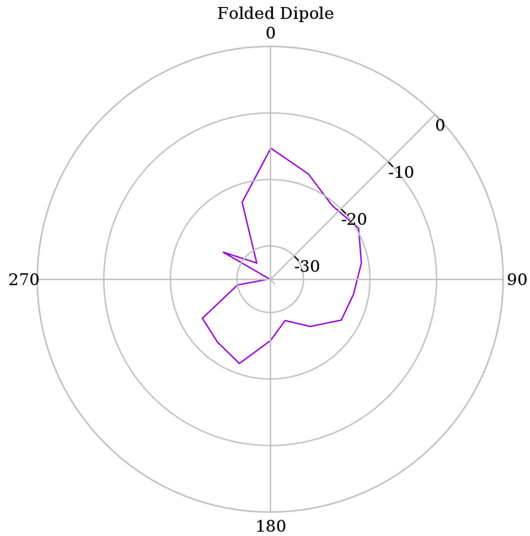

Fig. 10. Measured vertical radiation pattern at a distance of $4\,\text{m}$, where the signal is measured in dBFS

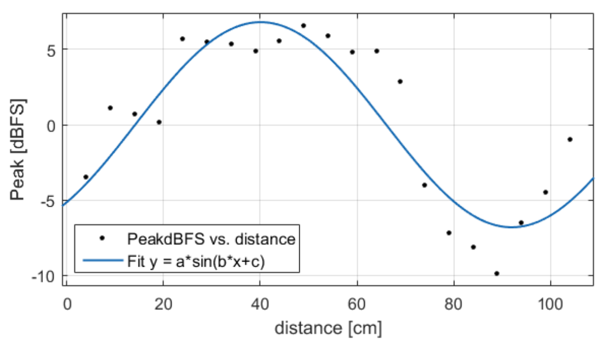

Fig. 11. Data point and sinusoidal fit of the peak vs distance while keeping the system 4 meters away from the receiver and varying s in steps of $5\,\text{cm}$

the corner reflector.

The experimenting was not flawless in its execution as a number of processing errors were made. While measuring the distances at which measurements were taken were not accurate. The dipole had to be manually held by a project team member meaning there was always a variation between the distances from the ground and corner reflector. As a result this produces a great number of inconsistencies.

In addition the electrical connection to the dipole was poorly connected and fragile. This many at times gave little or no signal and required constant repairing during the experiments which also contributed to the inconsistencies in the measurements taken.

In the second experiment where the corner reflector was added to compare with results from the initial experiment, the readings did improve but not as much as was expected. It is likely some of the waves passed through the reflector or reflected off the environment. This can be seen from the results above in section V-A where a signal from the antenna was still measured as the corner reflector pointed in the opposite direction. This reduces the effectiveness of the corner reflector.

In third experiment, the angles chosen were also difficult to measure because there was no reference point which contributed to inconsistencies. The experimental results of the rotational change have a rather large value related to its maximum value. For the sole dipole, this is a bit more than -20 dBFS against just less -20 dBFS. For the dipole with the corner reflector, this comes to -8 dBFS against -2 dBFS in the direction of the scale. The ideal distance between the corner reflector and the folded dipole seems to be $49\,\text{cm}$.

Some parts of the behaviour of the dipole can be explained by the way it was constructed. Too little attention was paid to the construction process and the challenges it brought with it. These challenges made us change the specifications of the dipole, which can be seen in Table I. These challenges included the soldering of the corner pieces of the dipole, but also connecting the coax cable to the dipole and the suspension of the dipole in the corner reflector.

VIII. Conclusion

The main aim of this report was to validate our design for the folded dipole antenna with a corner reflector through simulations and experiments. The SNR value seems to drop at some points, most notably the powers of 2 in terms of distance. The performance indicators like radiation intensity, directivity, gain, array factor and power coefficient were realized to a certain degree. The validity of these results in comparison to the simulations for the two rotation experiments have caused a large error margin because the back end seems to have a rather large reading as well, and the distance between the corner reflector and the folded dipole do not match up with the simulations as well. These experimental results do not seem to validate the calculations and simulations. The reasons for these inconsistencies in the report are attributed to the lack of experimental methodology and external environmental factors beyond our control such as interference with the outside world.

Acknowledgment

We would like to thank Prof. Dr. Ir. Gijs Krijnen for his valuable feedback throughout the various stages of the project and acknowledge Jorn Witteveen for his guidance too.

References

[1] N. Z. A. of Radio Transmitters (NZART), “Dipoles,” 2016.
[2] S. Gabriel, J. Jonker, J. van Liefland, N. Mathur, D. T. Nguyen, S. Oyediran, J. Ringoot, J. van der Schaaf, J. Schlief, and A. Veciana Picazo, *Antenna design*. 2016.
[3] G. Vetharatnam and A. Rashidifar, “Comparison between microstrip and dipole antenna backed by a corner reflector,” *Journal of Electromagnetic Waves and Applications*, vol. 29, no. 9, pp. 1194–1205, 2015.
[4] P. Bevelacqua, “The array factor,” 2016.
[5] R. Klopfenstein, “Corner reflector antennas with arbitrary dipole orientation and apex angle,” *IRE Trans. Antennas Propag.*, vol. 5, no. 3, pp. 297–305, 1957.
[6] J. Kraus, “The corner-reflector antenna,” *Proceedings of the IRE*, vol. 28, no. 11, pp. 513–519, 1940.
[7] J. J. Thomson, *Elements of the mathematical theory of electricity and magnetism*. University Press, 1909.
[8] R. P. Feynman, R. B. Leighton, and M. L. Sands, *The Feynman lectures on physics*. Addison-Wesley Pub. Co., 1963.
[9] A. Theory, “The friis equation,” 2015.
[10] Wikipedia, “Friis transmission equation,” 2016.